Ferroelectrics, 387:36–45, 2009

ISSN: 0015-0193 print / 1563-5112 online
DOI: 10.1080/00150190902966248

Low-Loss Perovskite Niobates $Ba(M^{2+}_{1/3}\ Nb_{2/3})O_3$: Composition, Structure, and Microwave Dielectric Properties

A. BELOUS,[1,*] O. OVCHAR,[1] O. KRAMARENKO,[1]
D. MISCHUK,[1] B. JANCAR,[2] M. SPREITZER,[2] D. SUVOROV,[2]
G. ANNINO,[3] D. GREBENNIKOV,[4] AND P. MASCHER[4]

[1]V.I.Vernadskii Institute of General and Inorganic Chemistry NAS of Ukraine, 32/24 Palladin Ave., Kyiv-142, 03680, Ukraine
[2]Jozef Stefan Institute, Jamova 39, 1000, Ljubljana, Slovenia
[3]Istituto per i Processi Chimico-Fisici, CNR., via G. Moruzzi 1, 56124 Pisa, Italy
[4]McMaster University, Hamilton, Ontario, L8S 4K1, Canada

A slight deviation from the compositional stoichiometry in both A-site and B-site deficient perovskites $Ba(M^{2+}_{1/3}\ Nb_{2/3})O_3$ (M – Co, Zn, Mg) was found to promote cation ordering processes in studied materials. The highest magnitudes of the Qxf product have been obtained in the non-stoichiometric BCN (Qxf = 90 000 GHz), and BMN (Qxf = 150 000–200 000 GHz). A significant "extrinsic" contribution to the microwave dielectric loss has been found in Co and Mg -containing perovskites. Possible structural factors responsible for the variation of the Q-factor in studied systems have been discussed.

Keywords Microwave dielectrics; complex perovskites; cation ordering; quality factor

1. Introduction

Dielectric materials with high permittivity (ε) and low dielectric loss (tg δ) in the microwave (MW) range are frequently used in the communication technique for the production of passive MW components like dielectric waveguides, mounting, dielectric antennas or dielectric resonators [1]. At the present time, with expanding working frequencies of wireless communications towards millimeter wavelength range, the extremely low dielectric loss in the MW range (high quality factor $Q = 1/\text{tg}\delta$) of a material becomes the main factor responsible for high selectivity of MW devices [1, 2]. During the last decades the complex perovskites $Ba(A^{2+}_{1/3}B^{5+}_{2/3})O_3$ (A^{2+} = Mg, Co, Zn; B^{5+} = Ta, Nb) have been generally considered as the most promising candidates to obtain the product $Q \times f \geq 100\ 000$ GHz [2–5]. The main characteristic feature of the high-Q perovskites $Ba(A^{2+}_{1/3}B^{5+}_{2/3})O_3$ is the presence of 1:2 ordered superstructure in their B-sublattice, which comprises single layers of A^{2+} cations alternating with double layers of B^{5+} cations perpendicular to the <111> direction of the pseudocubic cell [5–7]. It is well established that B-site cation ordering in complex

Received November 1, 2008; in final form February 6, 2009.
*Corresponding author. E-mail: belous@ionc.kar.net

perovskites has a significant influence on the dielectric losses (Q-factor) at microwave frequencies [7–9]. Usually, long-time sintering and annealing are required to ensure a high degree of the cation ordering in the perovskites $Ba(A^{2+}_{1/3}B^{5+}_{2/3})O_3$ [2–5, 7–9]. However, the ordering processes can be significantly promoted by the changes in chemical composition of a material, that is observed, for instance in $BaZrO_3$ doped $Ba(Zn_{1/3}Ta_{2/3})O_3$ (BZT) [7]. Davies et all have found that the formation of 1:2 ordered structure in these materials starts in small-size domains distributed in the disordered matrix [7]. They have shown the important role of Zr^{4+} in the stabilization of domain walls that facilitates ordering processes in a material, and hence improves its Q-factor magnitude. Similar improvement in the Q-factor has been also observed in the $Ba(Zn_{1/3}Nb_{2/3})O_3$ (BZN), and $Ba(Mg_{1/3}Nb_{2/3})O_3$ (BMN) perovskites with the non-stoichiometric composition, and ascribed to the enhancement of the ordering degree [9, 10]. However, excepting the BZN perovskites, the data related to the effect of compositional non-stoichiometry on the properties of 1:2 perovskites are often contradictory, and we are still far from the highest values of the Q-factor which can be obtained in the $Ba(A^{2+}_{1/3}B^{5+}_{2/3})O_3$ materials. Moreover, one may conclude that, in addition to the cation ordering other factors like lattice and microstructure defects or secondary phases may contribute to the Q- variation in the non-stoichiometric systems. This is especially relevant in the case of complex niobates $Ba(A^{2+}_{1/3}Nb_{2/3})O_3$ which generally demonstrate larger scattering in properties comparing to their tantalate based analogues.

Therefore, the main goal of this paper is to summarize and discuss some composition-derived changes in the microstructure, ordering degree, and the Q-factor of selected high-Q niobate based perovskites with the non non-stoichiometric composition.

2. Experimental Procedure

All studied materials have been produced by the conventional two-step mixed-oxide route. The starting reagents were extra pure MgO, Co_3O_4 (99.95%), Nb_2O_5 (99.9%), and $BaCO_3$ (99.9%). At the first stage the corresponding columbites $A^{2+}_{1+x}Nb_2O_6$ (A^{2+}–Mg,Co, Zn) have been synthesized. The calcinations temperatures of the mixtures ZnO-Nb_2O_5, Co_3O_4–$3Nb_2O_5$, and MgO-Nb_2O_5 have been chosen as 1000°C, 1150°C and 1200°C respectively. The soaking time was 4 hours. At the second stage the appropriate ratios of $BaCO_3$ and corresponding columbite were ball milled again, and calcined at 1150°C–1200°C for another 4 hours. The sintering was performed in air for 8 hours at the temperatures 1350°C–1500°C. The phase composition and crystal lattice parameters of sintered ceramics were examined by means of X-ray diffraction analysis (XRD) using CuKα–radiation (Model PW 1700, Philips, Eindhoven, The Netherlands). Microstructural analysis of the ceramic samples was performed by means of scanning electron microscopy (JEOL, JSM 5800, Tokyo, Japan) using energy dispersive X-ray spectroscopy (EDX) and the LINK software package (ISIS 3000, Oxford Instruments, Bucks, UK). Electron diffraction studies and TEM microscopic investigations of the foils were performed using a transmission electron microscope (JEOL 2000FX, JEOL, Tokyo, Japan) operating at 200 kV. Raman spectra were taken at room temperature on Renishaw 2000 spectrometer. 514 nm line of Ar^+ ion laser was used as an excitation source. The dielectric characteristics of the materials (ε , Q, and τ_f) at frequencies around 10 GHz were examined using a cavity reflection method on the Network Analyser PNA-L Agilent N5230A. In addition, the quality factor of studied materials was examined within the frequency range of 40–70 GHz by means of Whispering Gallery Mode (WGM) technique by a millimeter wave vector analyzer model 8–350-2 (courtesy of AB millimetre, Paris, France).

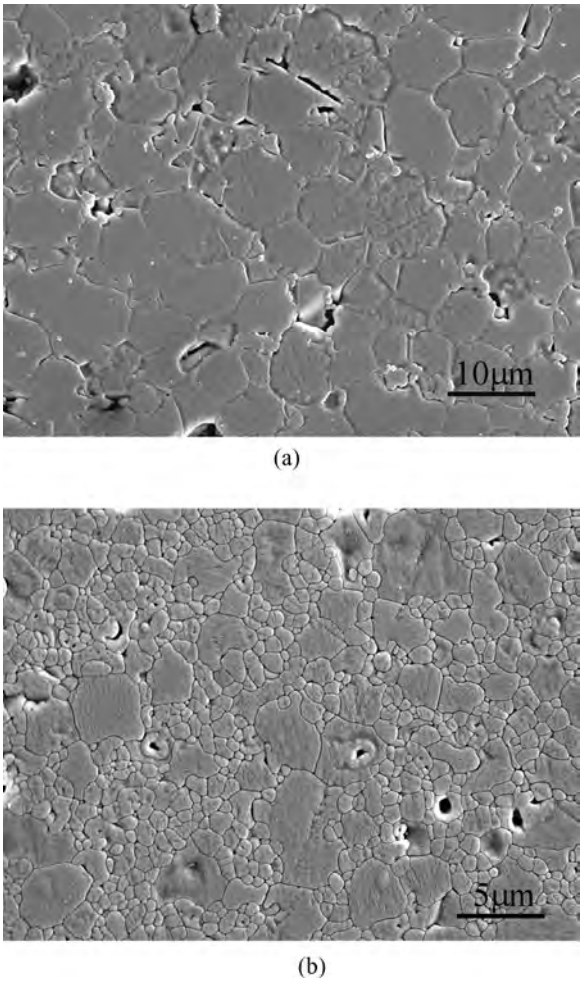

Figure 1. SEM microphotographs of the etched surface of $Ba_3Co_{1+x}Nb_2O_9$ samples sintered at 1470°C (8 h): (a) $x = 0$, (b) $x = -0.07$.

3. Results and Discussion

3.1. The system $Ba_3Co_{1+x}Nb_2O_9$

In this system we studied compositions corresponded to $-0.15 \leq x \leq 0.03$. Both XRD and SEM analyses of sintered ceramics denote the formation of a single-phase material at $-0.05 \leq x \leq 0.03$. At $x < -0.05$ the secondary phase $Ba_8CoNb_6O_{24}$ with the hexagonal perovskite structure is formed. These data have been also confirmed by more accurate WDS analysis. The increase in the amount of secondary phase with the Co-deficiency (decrease in x) is accompanied by a substantial decrease in the grain size of the ceramics (Fig. 1). For instance, at $x = -0.07$ -when only negligible amount of secondary $Ba_8CoNb_6O_{24}$ has been detected- the ceramics comprises grains with the irregular size distribution within the range of 0.5 to 7 μm. The changes in the ordering degree, which are not enough visible by XRD, are clearly seen from the electron diffraction patterns collected along [110] of the perovskite

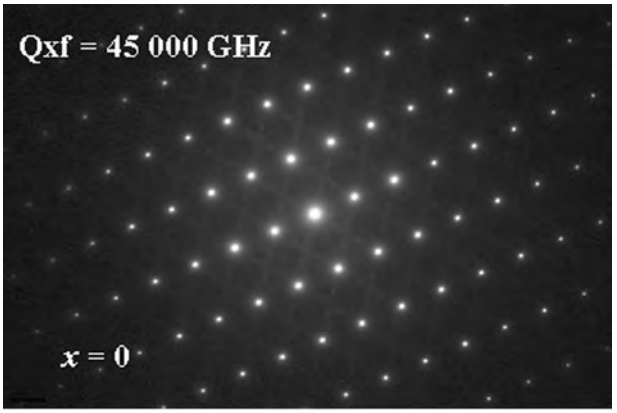

(a)

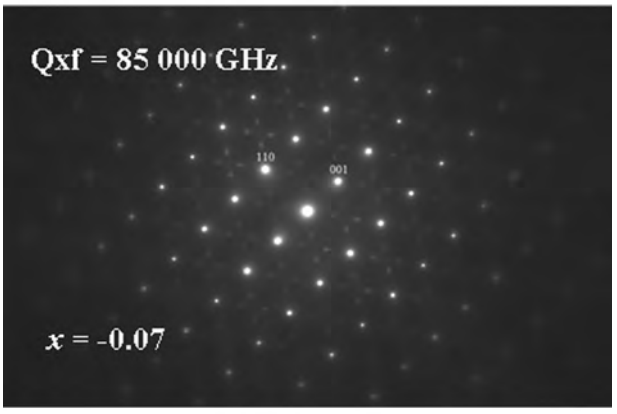

(b)

Figure 2. Electron diffraction patterns collected along [110] of the perovskite subcell of $Ba_3Co_{1+x}Nb_2O_9$ samples sintered at 1470°C (8 h): (a) $x = 0$, (b) $x = -0.07$.

subcell (Fig. 2). These data apparently demonstrate the increase in the 1:2 ordering degree with increasing Co-deficiency. In the stoichiometric $Ba_3Co_{1+x}Nb_2O_9$ (BCN) 1:2 cation ordering is at the initial stage which involves probably mixed 1:1 and 1:2 ordering motives (Fig. 2a). However, in the sample corresponding to $x = -0.07$ superlattice reflections at ($h \pm 1/3$, $k \pm 1/3$, $l \pm 1/3$) are observed along both <111> allowed directions (Fig. 2b). It should be noted that very similar results have bee reported by Davies et al for the BZT doped with 2.15% $BaZrO_3$ [7]. The authors of the Ref. 7 ascribed the observed data to the formation of a twinned ordered domain structure. In fact, Fourier transforms of the dark-field TEM images collected from the BCN ($x = -0.07$) denote the presence of the structure comprising domains with the average size of around 3–5 nanometers (Fig. 3). The further increase in the Co-deficiency ($x < -0.07$)–which is accompanied by increasing amount of secondary phase – does not result in any additional improvement in ordering. The electron diffraction data coincide also with the results obtained from the Raman spectra of non-stoichiometric BCN, in which we observe the decrease in the FWHM of the oxygen-octahedron stretch mode at 780 cm^{-1} (Fig. 4) indicating an increase in the 1:2 ordering [11].

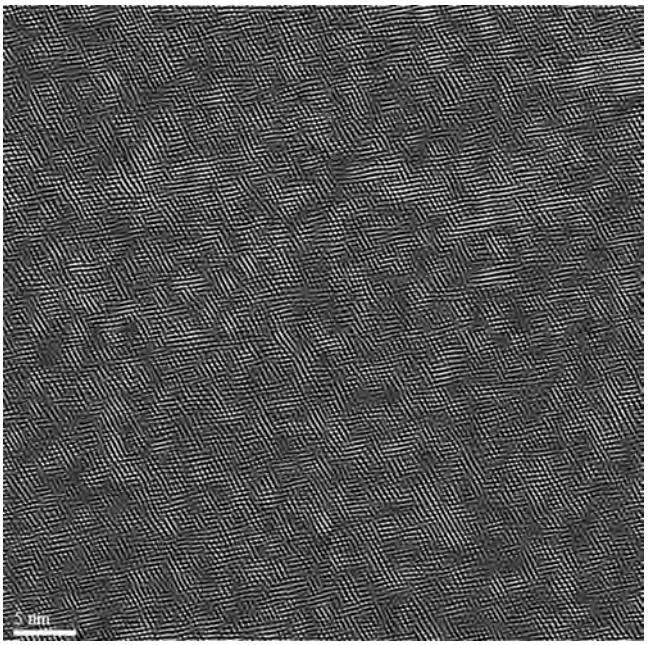

Figure 3. Fourier transform of the dark-field TEM image of $Ba_3Co_{0.93}Nb_2O_9$ ($x = -0.07$) samples sintered at 1470°C (8 h).

Most likely, the enhanced ordering in the Co-deficient BCN similarly to $BaZrO_3$ doped BZT originates from the formation of a stable nano-domain structure. Taking into account the fact that -according to TEM studies- the formation of secondary phase $Ba_8CoNb_6O_{24}$ starts at the grain boundaries of BCN, this Co-deficient phase inhibits the grain growth of the BCN material, and consequently contributes to the stabilization of the domain-structure.

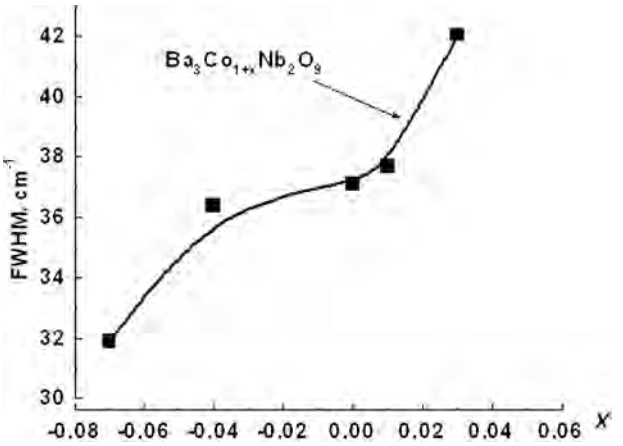

Figure 4. Variation of the FWHM of the oxygen-octahedron stretch mode at 780 cm^{-1} of $Ba_3Co_{1+x}Nb_2O_9$ as a function of Co content.

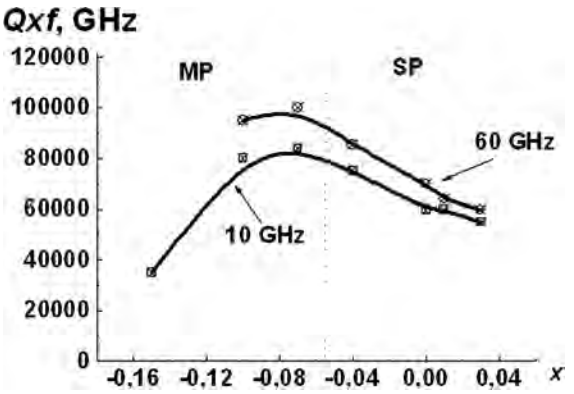

Figure 5. *Qxf* product of the samples $Ba_3Co_{1+x}Nb_2O_9$ as a function of Co content measured at the frequency 10 GHz and 60 GHz; MP- multiphase region, SP- single-phase region.

In accordance with the changes observed in the 1:2 ordering degree the Q-factor of Co-deficient BCN increases with decreasing x, and attains its maximum at around $x = -0.07$ when exactly the highest ordering degree was observed (Fig. 5). Therefore, from the experimental results we can state that the improved ordering in the Co-deficient BCN is the main factor responsible for the rise in the Q-factor. The decrease in Q which is observed at lower x – when no further ordering improvement is observed- is probably due to the increasing amount of secondary phase $Ba_8CoNb_6O_{24}$.

Therefore, increasing Co-deficiency as well as the consequent formation of Co-deficient perovskite $Ba_8CoNb_6O_{24}$ initiates at least two mechanisms with the opposite effect on the Q-factor of a material. On the one hand, the ordering process is improved that leads to increase in Q whereas on the other hand, the multiphase material is formed that leads to the decrease in Q. And, a superposition of these above mechanisms at $-0.1 \leq x \leq -0.05$ results in the appearance of the Q-maximum with the product $Q\mathrm{x}f$ as high as 85 000–90 000 GHz that is by 40–50% higher values measured in stoichiometric BCN. This conclusion is indirectly confirmed by the data of the WGM characterization of Co-deficient ceramics at the frequencies of around 60 GHz when the "external" processing-derived contribution to dielectric loss tends to diminish. At $-0.07 \leq x \leq 0.03$-when Q is preferably controlled by the 1:2 ordering degree- the increasing measurement frequency does not practically affect the behaviour of Q variation (Fig. 5). At the same time, in the 60 GHz range the Q-factor demonstrate rather weak dependence on increasing amount of $Ba_8CoNb_6O_{24}$ ($x < -0.07$). It should be noted that the maximum product $Q\mathrm{x}f$ measured at 60 GHz was even higher 100 000 GHz that allows one to estimate the contribution of extrinsic sources (including structural distortions, secondary phases, grain boundaries and micropores) into the dielectric loss as at least 20%. Therefore, we still have a possibility to improve the Q-factor of studied materials by the further optimization of sintering process.

3.2. The System $Ba_{3+3x}MgNb_2O_9$

When investigating non-stoichiometry in the Ba-subblatice of a BMN (the system $Ba_{3+3x}MgNb_2O_9$) x varied within the ranges $-0.15 \leq x \leq 0.05$. In this system the materials are well sintered only when $\mathrm{x} \leq 0$. With the further increase in x the sintering temperature sharply increased over 1600°C. In the case when $-0.01 \leq \mathrm{x} \leq 0$ sintered materials contain

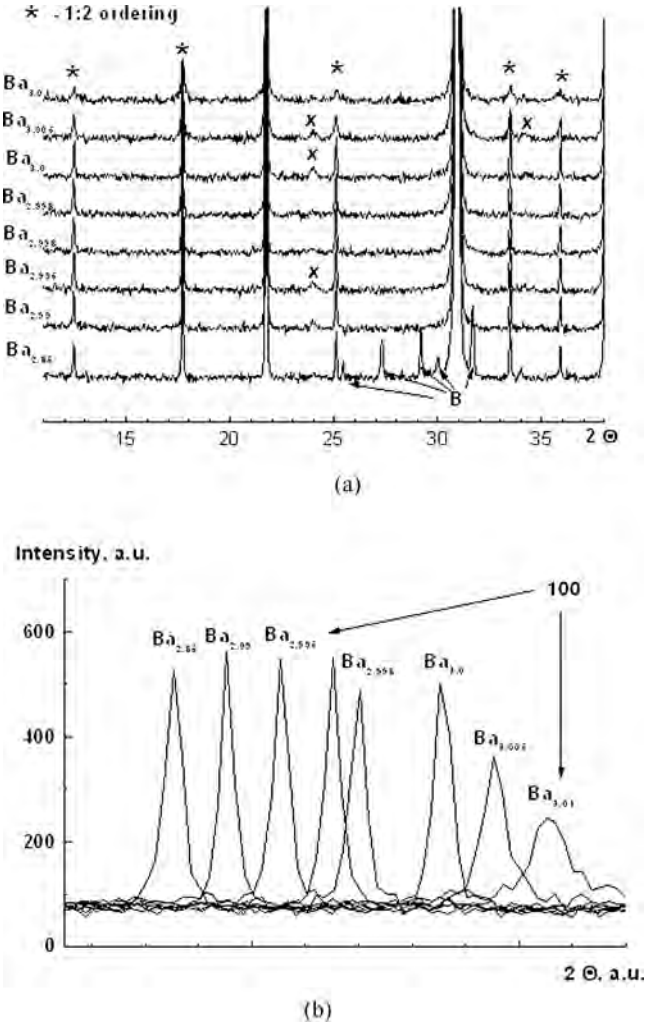

Figure 6. XRD patterns (a), and the comparison of the intensities of 1:2 ordering peak (100) on the arbitrary 2 theta axis (b) of the selected ceramics $Ba_{3+3x}MgNb_2O_9$ with different Ba content: B – Mg-containing analogue of ferroelectric $Ba_6CoNb_9O_{30}$; x –unknown phase.

only matrix perovskite phase BMN (Fig. 6a). At lower x new secondary phase appears whose peaks coincide with those of ferroelectric $Ba_6CoNb_9O_{30}$ with the tetragonal tungsten bronze (TTB) structure (Fig. 6a). However, this phase is hardly recognizable by SEM. The reason is that probably it is distributed at grain boundaries (because of its low melting temperature), and is pulled out when polished. In contrast to BCN and BZN perovskites all of the studied BMN materials demonstrate good ordering (Fig. 6a).

Similarly to the data obtained for the Co-deficient BCN, the microwave quality factor of BMN increases with increasing Ba-deficiency, and passes through maximum at $x = -0.01$ (Fig. 7). However, from XRD no clear relationship can be found between ordering degree and the product Qxf (Fig. 6b). One can only state that the ordering is suppressed with the increase in the Ba content ($x > 0$) (Fig. 6b) at equal other conditions. Therefore,

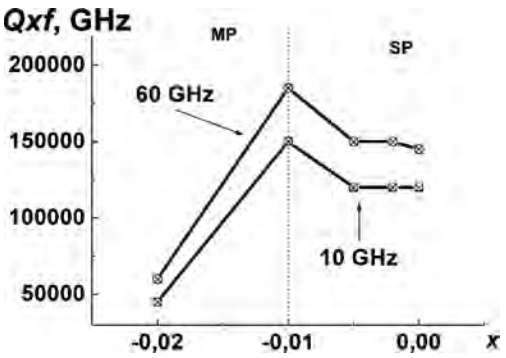

Figure 7. *Qxf* product of the samples $Ba_{3+3x}MgNb_2O_9$ as a function of Mg content measured at the frequency 10 GHz and 60 GHz; MP- multiphase region, SP- single-phase region.

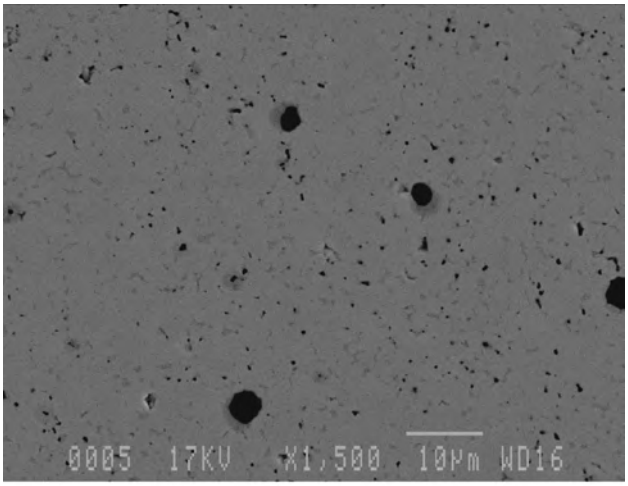

(a)

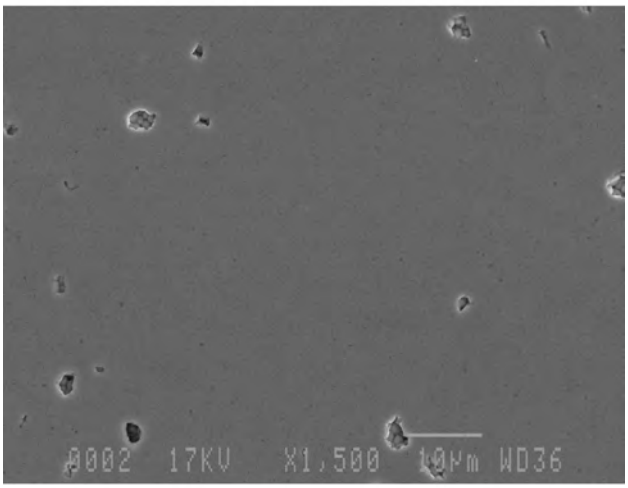

(b)

Figure 8. SEM microphotographs of the polished surface of $Ba_{3+3x}MgNb_2O_9$ (a) $x = 0$; (b) $x = -0.01$.

this question requires the further investigation. Probably, in the well ordered BMN the variation in Q can derive from the microstructural characteristics. In fact, our preliminary results show that the less porous structure (Fig. 8b) corresponds to the highest product Qxf of 150 000 GHz. At the same time Qxf as high as 120 000 GHz has been obtained in highly porous ceramics with stoichiometric composition (Fig. 8a). It should be also noted that at the frequency of around 60 GHz the product Qxf of Ba-deficient BMN ($x = -0.01$) was as high as 185 000 GHz that correspond to the maximum values of the Q-factor which can be obtained in this system.

Deriving from the already obtained results it is possible to define several competing factors which are mainly responsible for the variation of the Q-factor in non-stoichiometric BMN materials $Ba_{3+x}MgNb_2O_9$ namely (a) high degree of 1:2 cation ordering, and (b) the formation of undesirable secondary phase (Mg-containing analogue of ferroelectric $Ba_6CoNb_9O_{30}$). And, the effect of the latter factor can in many cases prevail over the effect of ordering process.

4. Conclusions

The microstructure, phase composition and the microwave quality factor of the perovskites $Ba(A^{2+}_{1/3}Nb_{2/3})O_3$ (A^{2+} = Co, Mg) are to a large extent effected by a deviation from stoichiometric composition. In the non-stoichiometric BCN the deficiency in Co initiates at least two mechanisms with the opposite effect on the Q-factor of a material: improved ordering that leads to increase in Q, and formation of multiphase material that leads to the decrease in Q. A superposition of these competing mechanisms at $-0.1 \leq x \leq -0.05$ results in the appearance of the Q-maximum with the product Qxf as high as 85 000–90 000 GHz that is by 40–50% higher values measured in stoichiometric BCN. Measurement of the Q-factor of Co-deficient BCN over the wide frequency ranges allowed us to estimate the contribution of extrinsic sources (including structural distortions, secondary phases, grain boundaries and micropores) into the dielectric loss as at least 20%. In the Ba-deficient BMN the Q-factor is determined by the competing effect of the improved 1:2 ordering and the formation of small-size inclusions of the ferroelectric phase with tetragonal tungsten bronze As a consequence, the highest magnitudes of the Qxf product have been obtained in the Co-deficient BCN (Qxf = 90 000–100 000 GHz) and in Ba-deficient BMN (Qxf = 150 000–185 000 GHz).

Acknowledgments

This work was partially supported by the NATO Grant under the NATO SfP project 980881: "Dielectric Resonators" of the NATO "Science for Peace" Program.

References

1. W. Wersing, Microwave ceramics for resonators and filters. *Curr. Opin. Solid State Mater. Sci.* **1**, 715–731 (1996).
2. S. J. Fiedziuszko, I. C. Hunter, T. Itoh, Y. Kobayashi, T. Nishikawa, S. N. Stitzer, and K. Wakino, Dielectric materials, devises, and circuits. *IEEE Trans. Microwave Theory Technol.* **MTT-50**, 706–720 (2002).
3. S. Kawashima, M. Nishida, I. Ueda, H. Ouchi, and S. Hayakawa, Dielectric properties of Ba(Zn,Ta)O –Ba(Zn,Nb)O ceramic. *Proc. Ferroelect. Mater. Applicat.* **1**, 293–296 (1977).

4. H. Matsumoto, H. Tamura, and K. Wakino, Ba(Mg,Ta)O_3-$BaSnO_3$ high-Q dielectric resonator. *Jpn. J. Appl. Phys.* **30**, 2347–2349 (1991).
5. F. Galasso and J. Pyle, Ordering of the compounds of the A(B'$_{0.33}$Ta$_{0.67}$)O_3 type. *Inorg. Chem.* **2**(3), 482–484 (1963).
6. T. Takahashi, E. J. Wu, A. Van Der Ven, and G. Ceder, First-principles Investigation of B-site ordering in Ba(Mg_xTa_{1-x})O_3 microwave dielectrics with complex perovskite structure. *Jpn. J. Appl. Phys.* **39**, 1241–1247 (2000).
7. P. K. Davis, J. Tong, and T. Negas, Effect of ordering-induced domain boundaries on low-loss Ba($Zn_{1/3}Ta_{2/3}$)O_3–$BaZrO_3$ perovskite microwave dielectrics. *J. Am. Ceram. Soc.* **80**(7), 1724–1740 (1997).
8. F. Azough, C. Leach, and R. Freer, Effect of nonstoichiometry on the structure and microwave dielectric properties of Ba($Co_{1/3}Nb_{2/3}$)O_3 ceramics. *J. Eur. Ceram. Soc.* **26**(14), 2877–2884 (2006).
9. H. Wu and P. K. Davies, Influence of non-stoichiometry on the structure and properties of Ba($Zn_{1/3}Nb_{2/3}$)O_3 microwave dielectrics: II. Compositional variations in Pure BZN. *J. Am. Ceram. Soc.* **89**(7), 2239–2249 (2006).
10. J. H. Paik, I. T. Kim, J. D. Byun, H. M. Kim, and J. Lee, The effect of Mg deficiency on the microwave dielectric properties of Ba($Mg_{1/3}Nb_{2/3}$)O_3 ceramics. *J. Mat. Sci. Letters.* **17**, 1777–1780 (1998).
11. C.-T., Chia, Y.-C. Chen, H.-F. Cheng, and I.-N. Lin, Correlation of microwave dielectric properties and normal vibration modes of xBa($Mg_{1/3}Ta_{2/3}$)O_3–(1–x)Ba($Mg_{1/3}Nb_{2/3}$)O_3 ceramics: I. Raman spectroscopy. *J. Appl. Phys.* **94**, 3360–3364 (2003).